Microwave-assisted synthesis: A fast and efficient route to produce $LaMO_3$ (M = Al, Cr, Mn, Fe, Co) perovskite materials

J. Prado-Gonjal, Á.M. Arévalo-López, E. Morán *

Departamento de Química Inorgánica, Facultad de Ciencias Químicas, Universidad Complutense de Madrid, 28040 Madrid, Spain

A B S T R A C T

A series of lanthanum perovskites, $LaMO_3$ (M = Al, Cr, Mn, Fe, Co), having important technological applications, have been successfully prepared by a very fast, inexpensive, reproducible, environment-friendly method: the microwave irradiation of the corresponding mixtures of nitrates. Worth to note, the microwave source is a domestic microwave oven. In some cases the reaction takes place in a single step, while sometimes further annealings are necessary. For doped materials the method has to be combined with others such as sol–gel. Usually, nanopowders are produced which yield high density pellets after sintering. Rietveld analysis, oxygen stoichiometry, microstructure and magnetic measurements are presented.

Keywords:
A. Oxides
A. Inorganic compounds
B. Chemical synthesis
B. Magnetic properties
C. X-ray diffraction
C. Thermogravimetric analysis
D. Crystal structure

1. Introduction

Lanthanum perovskites ($LaMO_3$) containing metals of the first transition series are very appealing functional materials because of their immense technological potential: some of them are used as components for solid oxide fuel cells (SOFCs), others are very efficient catalysts, some are used as membranes for separation processes or as gas sensors in automobiles, several show magneto-optic or magnetoresistant properties, and so forth; moreover some of these materials, where different properties coexist, are multifunctional [1–3]. In the case of $LaAlO_3$ it is a well-known substrate for depositing superconducting thin films because of its excellent lattice and thermal expansion matching with 1–2–3 superconductors. These materials are usually synthesized by the traditional solid state method at high temperatures (>1000° C) for extended periods, and by means of other chemical methods, such as sol–gel [4], citrate complexation [5], combustion [6], hydrothermal [7] and so on, but their synthesis using microwave radiation in a reproducible way is quite scarce and just a few authors have reported partial studies [8–11]. However, the possibility of processing ceramic materials with microwave energy is not recent: In 1975, Sutton observed that microwaves were able to heat the ceramic materials [12]. Nowadays, this method of synthesis of inorganic compounds, which enhance the rate of formation of ceramics by several orders of magnitude – therefore a "Fast Chemistry" route –, and which may induce interesting changes in morphology and sizes, is becoming an attractive field of research [13–15]. In our opinion, it is specially worth to recall the pioneering work – in the latest 80s – by Mingos et al. showing the possibility to produce advanced ceramic materials by using microwaves [16–18] as well as a comprehensive review published in 1999 by Rao et al. [19].

Worth to note, microwaves are electromagnetic radiation in the frequency range between 300 GHz to 300 MHz (2.45 GHz frequency are used almost universally for domestic ovens) and can be absorbed by ceramic either through polarization or conduction processes. Polarization involves short-range displacement of charge through formation and rotation of electric dipoles. Conduction requires long-range transport of charge [20]. For materials that are fairly susceptive to microwaves, the kinetics of microwave synthesis can be much faster than in a conventional process [21]. The electromagnetic field polarizes dipolar substances which induces a dipole in the molecule. As a result increased rotation sets in which causes internal heating of the substance which is proportional to the dielectric constant of the

* Corresponding author.
E-mail address: emoran@quim.ucm.es (E. Morán).

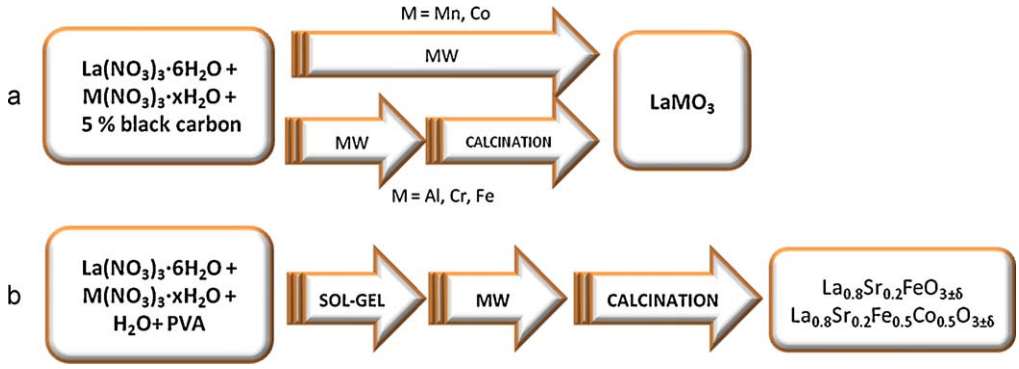

Fig. 1. Microwave routes followed to produce different lanthanum perovskites.

material, where the average microwave power absorbed [P] by the material (W/m^3) can be calculated with the expression:

$$P = \text{Electric losses} + \text{magnetic losses} = \omega\varepsilon_o\,\varepsilon''_{eff}E^2_{rms} + \omega\mu_o\mu''_{eff}\;H^2$$

where ω is the angular frequency, ε_o is the permittivity of free space ($\varepsilon_o = 8.854 \times 10^{-12}$ F/m), ε''_{eff} is the effective relative dielectric loss factor ($\varepsilon''_{eff} = \varepsilon''_{polarisation} + \varepsilon''_{condition}$), E_{rms} refers to the root mean square of the electric field, μ_o corresponds to the permeability of free space ($\mu_o = 4\pi \times 10^{-7}$ H/m), μ_{eff} is the effective relative loss factor ($\mu''_{eff} = \mu''_{polarisation} + \mu''_{condition}$) and H_{rms} refers to the root mean square of the magnetic field [22,23].

The heat produced by these mechanisms may produce – locally – very high temperatures (~1000 °C) [8] able to decompose some reactants and promote the expected reactions. In this connection, hydrated metal nitrates are appropriate precursors for this kind of reactions: their quite high relative dielectric constants (between 18 and 25) help to absorb effectively microwave radiation resulting in internal heating and decomposing. The reaction is effective and fast. However, sometimes it has to be used a secondary heater such as black carbon, graphite, SiC and so on, to help precursors to couple with microwaves and to scatter the radiation in all directions [24,25].

Thus, the aim of this work is to produce some important lanthanum perovskites – $LaMO_3$ (M = Al, Cr, Mn, Fe, Co) – by microwave irradiation of the corresponding mixtures of nitrates. All these materials are well-known in the literature because of their extraordinary and different physical properties and, on the other hand, to synthesize two different doped perovskites, $La_{0.8}Sr_{0.2}FeO_3$ and $La_{0.8}Sr_{0.2}Fe_{0.5}Co_{0.5}O_3$, used as cathodes in SOFC's by combining microwaves with a sol–gel method, demonstrating that these methods of synthesis are extraordinarily simple, efficient, yielding products of excellent crystallinity. Here, we report our analysis on the structure and properties of these perovskites, with particular emphasis on the phases directly produced by microwave solid state synthesis.

2. Experimental

2.1. Synthesis

Metal nitrates were used as starting materials. The equimolar amounts of metal nitrates were weighed according to the nominal composition of $LaMO_3$ (M = Al, Cr, Mn, Fe, Co). Nitrates were mixed with 5% weight of carbon black, which was added to enhance microwave absorption, and then mechanically homogenized and compacted in pellets of 13 mm diameter. The pellets were put in a porcelain crucible and placed inside another larger one stuffed with mullite. Worth to note, the microwave source is a domestic oven, operating at 2.45 GHz frequency and 800 W power and, in order to avoid damages, a beaker with a large amount water was maintained inside during the experiment. $LaCoO_3$ and $LaMnO_3$ materials were directly obtained after 30 min of irradiation while for $LaAlO_3$, $LaCrO_3$ and $LaFeO_3$ following the microwave irradiation, it is necessary a second step, heating in air in a conventional furnace at different temperatures (500 °C for $LaFeO_3$, 850 °C for $LaCrO_3$ and 1000 °C for $LaAlO_3$). To prepare doped materials, $La_{0.8}Sr_{0.2}FeO_3$ and $La_{0.8}Sr_{0.2}Fe_{0.5}Co_{0.5}O_3$, it is necessary to combine the described microwave method with sol–gel methodology. The

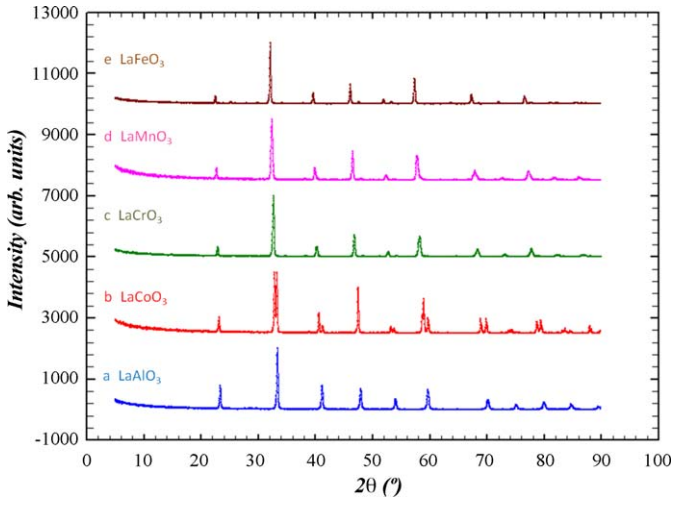

Fig. 2. X-ray diffraction patterns of undoped lanthanum perovskites.

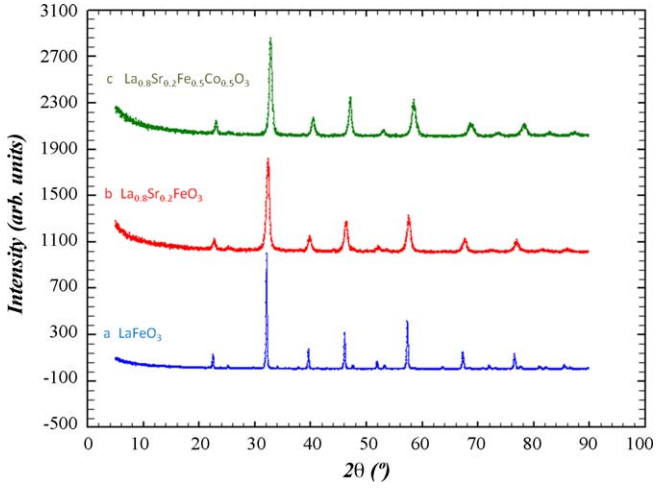

Fig. 3. X-ray diffraction patterns of lanthanum ferrites. All of them are nanometric (Debye–Scherrer particle sizes range between 7 and 35 nm).

sol–gel process followed is similar to that reported in Ref. [26]. The equimolar amounts of metal nitrates were dissolved in distilled water and a saturated polyvinyl alcohol (PVA) (Fluka, 98%) solution was added as the complexing agent. The amount of PVA added was such that the ratio of total number of moles of cations to that of PVA was 1:2. Then the final solution was maintained at 80 °C for 3 h to remove water and a viscous solution – gel – was formed. This gel was irradiated with microwaves – as described previously – during 30 min. This polymeric and sponge-like-precursor was calcined in air at 500 °C for 2 h in order to decompose the organic remnants, rendering a black powder as final product. The scheme of the synthesis is summarized in Fig. 1.

2.2. Characterization

Powder X-ray diffraction data (XRD) were collected on a Philips X'Pert PRO ALPHA1 of Panalytical B.V. diffractometer with Cu Kα1 monochromatic radiation (λ = 1.54056 Å) at room temperature equipped with a primary curved Ge111 primary beam monochromator and a speed X'Celerator fast detector. For cell parameters measurements and phase identification, the angle step and the counting time were respectively 0.017° (2θ) and 9 s. Fullprof software was retained XRD Rietveld refinement. The oxygen content was determined by thermogravimetric analysis (TGA) on a Cahn D-200 electrobalance on samples of about 50 mg in a H_2 (200

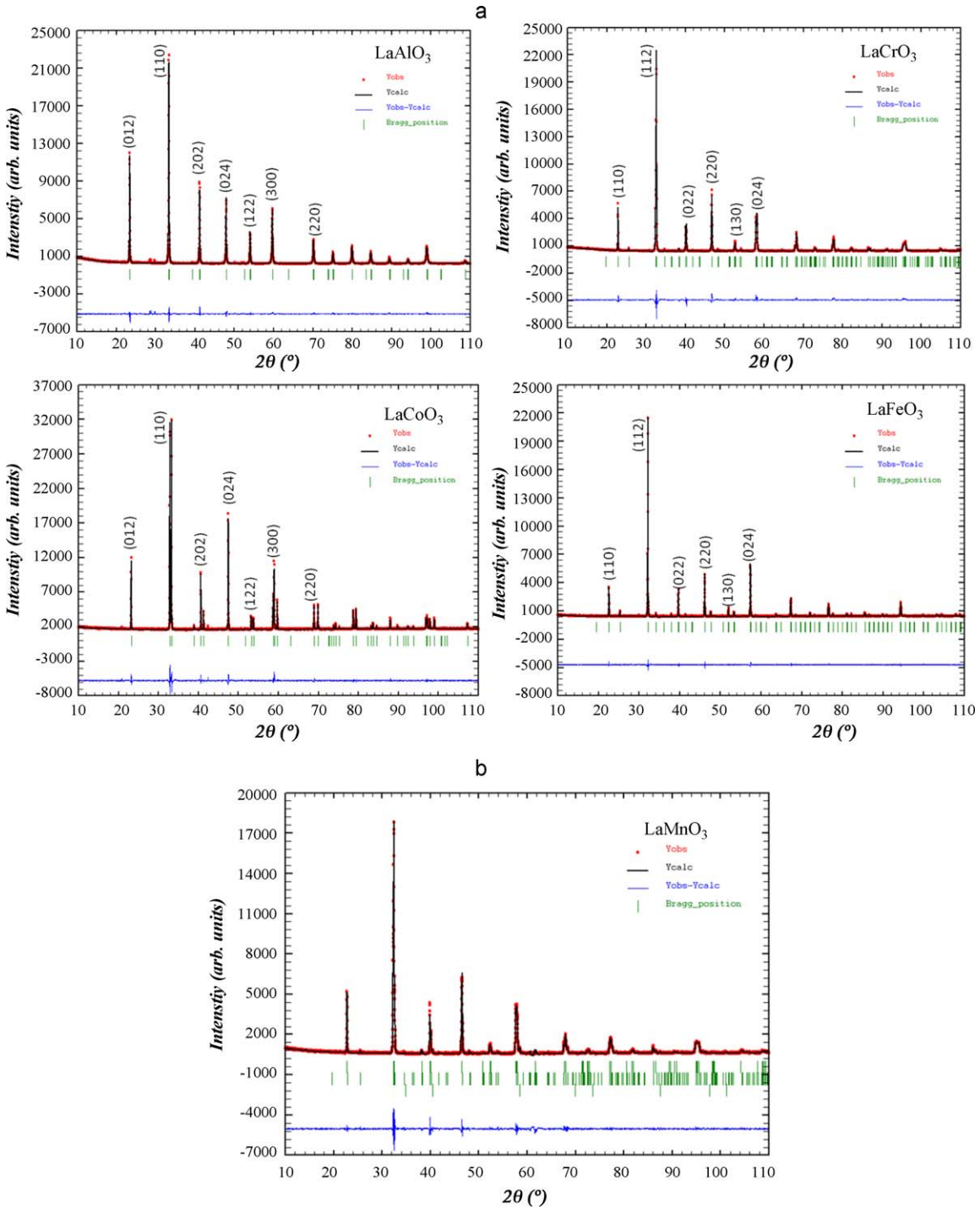

Fig. 4. Rietveld refinements: Observed and calculated diffraction patterns.

mbar)/He (400 mbar) atmosphere heating until 700 °C at 6 °C/min ratio. Samples were also examined by scanning electron microscopy (SEM) on a Jeol 6400 microscope equipped with an EDAX Inc. energy-dispersive X-ray detector for microanalysis, and selected area electron diffraction (SAED) was performed in a Jeol-2000FX electron microscope operating at 200 kV. The value of the specific area of $LaMnO_3$ was measured by the BET method and calculated from the corresponding nitrogen adsorption isotherms at 77 K, using a Micrometrics ASAP 200 surface analyzer. Magnetic susceptibility measurements were performed in a Quantum Design XL-SQUID magnetometer in the temperature range of 2–300 K at 1000 Oe magnetic field.

3. Results and discussion

3.1. Synthesis aspects and structural characterization

For $LaAlO_3$ and $LaFeO_3$ the microwave described method yields an amorphous powder after 10 min of microwave irradiation, however, after a further annealing in air at 500 °C for 24 h, the samples become crystalline. For chromium, two different phases can be obtained by microwave assisted synthesis: $LaCrO_4$ is produced when the sample is heated at 500 °C and $LaCrO_3$ when the calcination is performed at 850 °C. Otherwise, 30 min of microwave irradiation are sufficient to get pure and crystalline $LaMnO_3$ and $LaCoO_3$ materials without any additional thermal treatment. This seems to be due to the metallic character of $LaMnO_3$ and $LaCoO_3$ which play a similar role to that played by the black carbon added as susceptor: in these cases, the first nuclei produced by microwave absorption do scatter the radiation and speed up the reaction until completion. On the other hand, for $La_{0.8}Sr_{0.2}FeO_3$ and $La_{0.8}Sr_{0.2}Fe_{0.5}Co_{0.5}O_3$, the microwave heating does not proceed in the same way as for the other samples and, even longer times of microwave irradiation (up to 2 h), do not yield crystalline materials. Although the method has many advantages, it presents some drawbacks too, and it has to be pointed out that the lack of temperature control is the biggest handicap for this kind of synthesis if using a domestic microwave oven.

The XRD patterns of the simple perovskites – Fig. 2 – present the basic reflections corresponding to the perovskite structure and all the Bragg reflections of the materials can be indexed by comparison with the respective JCPDS cards. It can be observed, for $LaCrO_3$, $LaMnO_3$ and $LaFeO_3$, all of them crystallizing in the *Pbnm* space group, a displacement of the main peaks towards lower angles, the expected trend for chromium and iron but slightly different for manganese, taking into account the respective high spin ionic radii $^{VI}Cr^{3+}$: 0.615 Å, $^{VI}Mn^{3+[HS]}$: 0.65 Å, and

Table 1
Unit cell parameters and agreement factors, obtained through Rietveld analysis,.

	Point group	*a* (Å)	*b* (Å)	*c* (Å)	*V* (Å^3)	R-factors
$LaAlO_3$	R3c	5.36444 (4)	5.36444 (4)	13.1195 (2)	326.961 (6)	Rp: 4.62 Rwp: 5.95 Rexp: 4.56 χ^2: 1.70
$LaCoO_3$	R-3c	5.44366(2)	5.44366 (2)	13.09569(5)	336.079 (2)	Rp: 2.45 Rwp: 3.65 Rexp: 2.24 χ^2: 2.67
$LaCrO_3$	Pbnm	5.51632 (6)	5.47895 (6)	7.76161 (9)	234.584(5)	Rp: 3.53 Rwp: 4.63 Rexp: 4.09 χ^2: 1.28
$LaFeO_3$	Pbnm	5.55623 (4)	5.56304 (4)	7.85346 (6)	242.747 (3)	Rp: 3.53 Rwp: 4.60 Rexp: 4.36 χ^2: 1.11
$LaMnO_3$	R-3c /Pbnm	5.5312 (1)/5.5397 (2)	5.5312 (1)/5.4891 (1)	13.488(6)/7.7928 (3)	357.27 (2)/236.96 (1)	Rp: 6.59 Rwp: 10.2 Rexp: 3.67 χ^2: 7.74

Table 2
Atomic positions, as deduced from the Rietveld analysis,.

		x	*y*	*z*
$LaAlO_3$	La	0.0000	0.0000	0.2500
R3c	Al	0.0000	0.0000	0.0000
	O	0.5250(1)	0.0000	0.2500
$LaCoO_3$	La	0.0000	0.0000	0.2500
R-3c	Co	0.0000	0.0000	0.0000
	O	0.549(1)	0.0000	0.2500
$LaCrO_3$	La	0.9979(9)	0.0164(4)	0.2500
Pbnm	Cr	0.5000	0.0000	0.0000
	O1	0.083(3)	0.498(4)	0.2500
	O2	0.228(3)	0.221(3)	0.537(2)
$LaFeO_3$	La	0.0193(8)	0.0281(2)	0.2500
Pbnm	Fe	0.0000	0.5000	0.0000
	O1	0.091(3)	0.488(2)	0.2500
	O2	−0.289(4)	0.290(4)	0.029(2)
$LaMnO_3$	La	0.0183(7)/0.0000	0.5179/0.0000	0.2500
Pbnm/R3c	Mn	0.0000	0.0000	0.0000
	O1	−0.004(7)/0.5514(8)	−0.008(6)/0.0000	0.2500
	O2	/0.797(9)	/0.289(8)	/−0.002(8)

$^{VI}Fe^{3+[HS]}$: 0.645 Å [27]. In this connection, it is worth to recall the high structural complexity of $LaMnO_3$, as discussed below. $LaAlO_3$ and $LaCoO_3$ although crystallizing in similar space groups, *R*3*c* and *R*-3*c* (hexagonal setting), respectively, show very different diffraction patterns owing to the fact that Co^{3+}, as we will discuss later, may be in high, low or intermediate spin. Concerning the iron-containing perovskites, in Fig. 3, we show the diffraction patterns corresponding to the undoped and two strontium-doped materials. It can be observed a shift to higher angles of the diffraction maxima, corresponding to smaller parameters, contrary to the expected shift knowing the respective ionic radii of $^{VIII}La^{3+}$: 1.18 Å and $^{VIII}Sr^{2+}$: 1.25 Å [27] but which can be explained taking into account the presence of some Fe^{4+} induced by doping. Worth noting, the doped samples remain nanocrystalline even after being calcined at 1000 °C, as can be inferred from the width of the diffraction maxima if compared to the undoped ferrite.

Crystal structure refinement has been carried out by Rietveld analysis. Fig. 4 shows the observed and calculated diffraction patterns. The results obtained for $LaMO_3$ (M = Al, Cr, Fe and Co) concerning cells parameters and atomic positions are in very good agreement with the values reported in the literature [28–31] as indicated by the *R*-factors which are summarized in Tables 1 and 2. Nevertheless, for the lanthanum manganite the agreement factors are not so good, and the Rietveld analysis shows the coexistence of two different phases crystallizing in the *R*-*3c* and *Pbnm* space groups, respectively, as already observed by Wold and Arnott in 1959 who suggested a phase transition is taking place, from orthorhombic structure to rhombohedral at ~600 °C [32]. Worth to

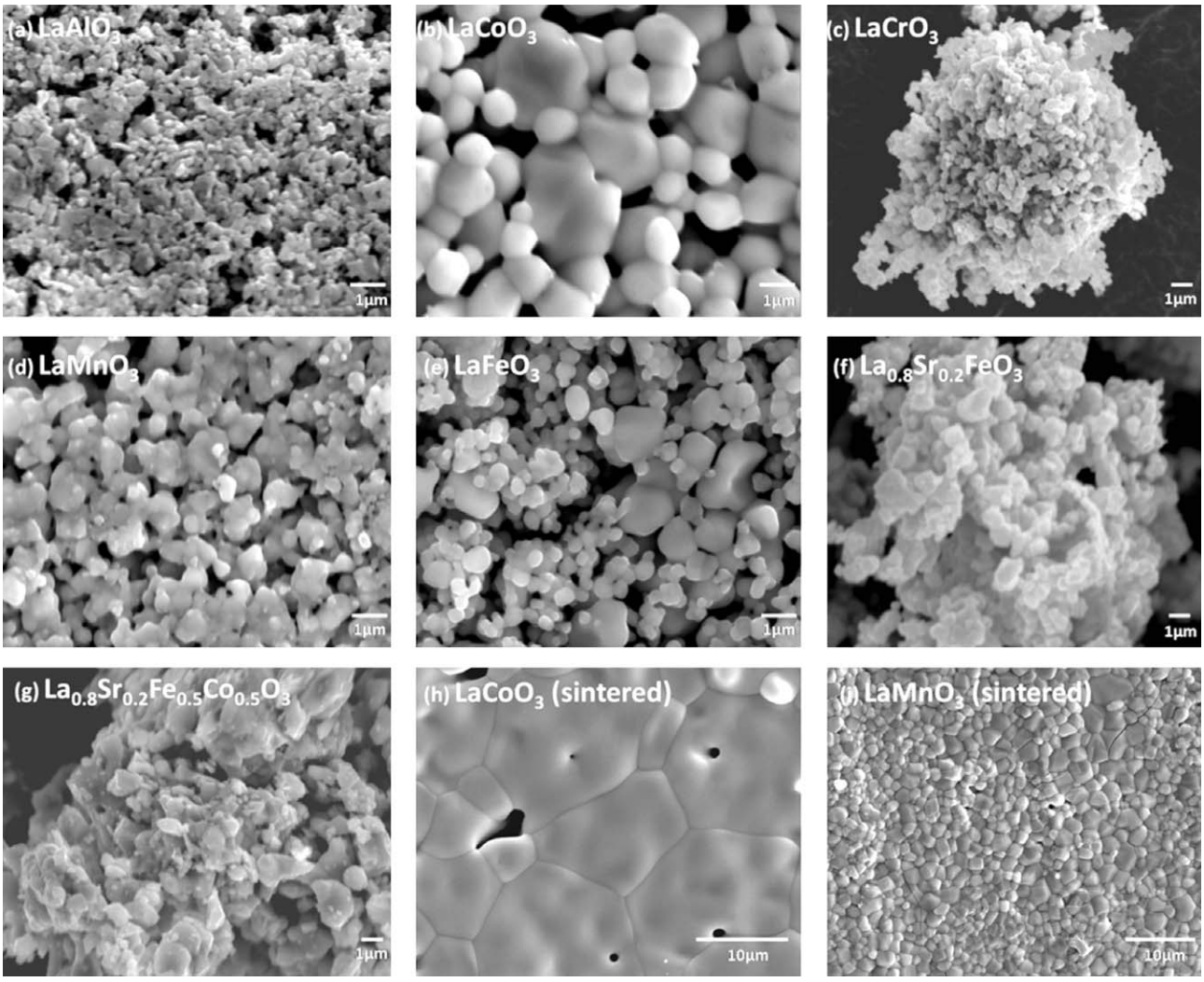

Fig. 5. SEM micrographs of lanthanum perovskites. (a–g): as prepared polycrystalline powders; (h,i): pellets sintered at 1300 °C.

Table 3
EDS analysis (atomic %) for Lanthanum perovskites ($LaMO_3$).

	$LaAlO_3$	$LaCoO_3$	$LaCrO_3$	$LaMnO_3$	$LaFeO_3$	$La_{0.8}Sr_{0.2}FeO_3$	$La_{0.8}Sr_{0.2}Fe_{0.5}Co_{0.5}O_3$
Al	20.2						
Co		21.2					9.6
Cr			19.1				
Fe					20.4	17.2	9.6
La	18.9	22.6	19.3	23.7	20.7	14.4	16.1
Mn				21.4			
Sr						3.9	4.8

Ideal values are 20% both in the La and the M perovskite positions.

be noted, our results correspond to samples heated at 1000 °C and therefore, this is not a temperature-induced phase transition and the phase coexistence seems to reflect failure to control stoichiometry during heating. The literature is plenty of data concerning lanthanum manganites, doped or not, and there is general agreement about the intrinsic complexity of these materials [33]: Mn^{3+}/Mn^{4+} mixed valence, oxygen hyperstoichiometry or cationic vacancies, different symmetries, etc. It has been demonstrated that the usual notation "$LaMnO_{3+\delta}$", which would indicate excess [interstitial] oxygen in the lattice, does not represent the real unit cell, the real formula should be written as $La_{1-\varepsilon}Mn_{1-\varepsilon}O_3$ (with $\varepsilon = \delta/[3 + \delta]$), a notation which indicates a fully occupied oxygen lattice, showing, however, cation vacancies [34].

3.2. Microstructure analysis

Fig. 5 shows the SEM micrographs corresponding to lanthanum perovskites. The micrographs clearly indicate the agglomeration of polyhedral particles of submicronic or nanometric size, with the exception of $LaCoO_3$ in which crystals are much bigger. These features are important for processing at higher temperatures in order to fabricate devices and, just to give representative examples, in this figure two samples ($LaMnO_3$ and $LaCoO_3$) sintered in air at 1300 °C are shown: very compact, void-free and, consequently, high density pellets can be produced. Regarding chemical analysis, the metallic proportions as detected from EDS are very close to the nominal ones and appear in Table 3 This implies that the distributions of elements in the bulk materials are rather homogeneous.

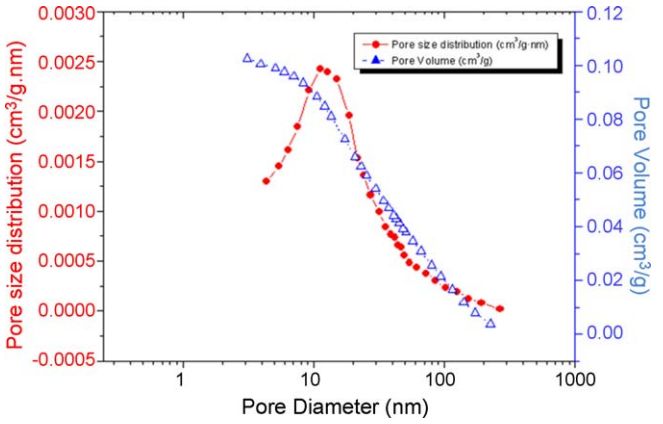

Fig. 6. Pore size distribution (cm^3/g nm) and pore volume (cm^3/g) for $LaMnO_3$ as deduced from the N_2 isotherm at 77 K.

For $LaMnO_3$, which is the sample with smaller particle size (nanosized as seen by TEM, see below) BET analysis has been performed and shows a specific surface area of 17.65 ± 0.04 m^2/g, in good agreement with the results obtained by other methods of synthesis [35]. We note that the Nitrogen absorption isotherm corresponds to type IV, a typical isotherm for mesoporous compounds. The measured pore size distribution is shown in Fig. 6, a quite narrow peak, pointing to a very homogeneous material with an average pore size of about 12 nm.

TEM images performed with the starting powders, that are perovskites obtained at the lowest possible temperatures, show

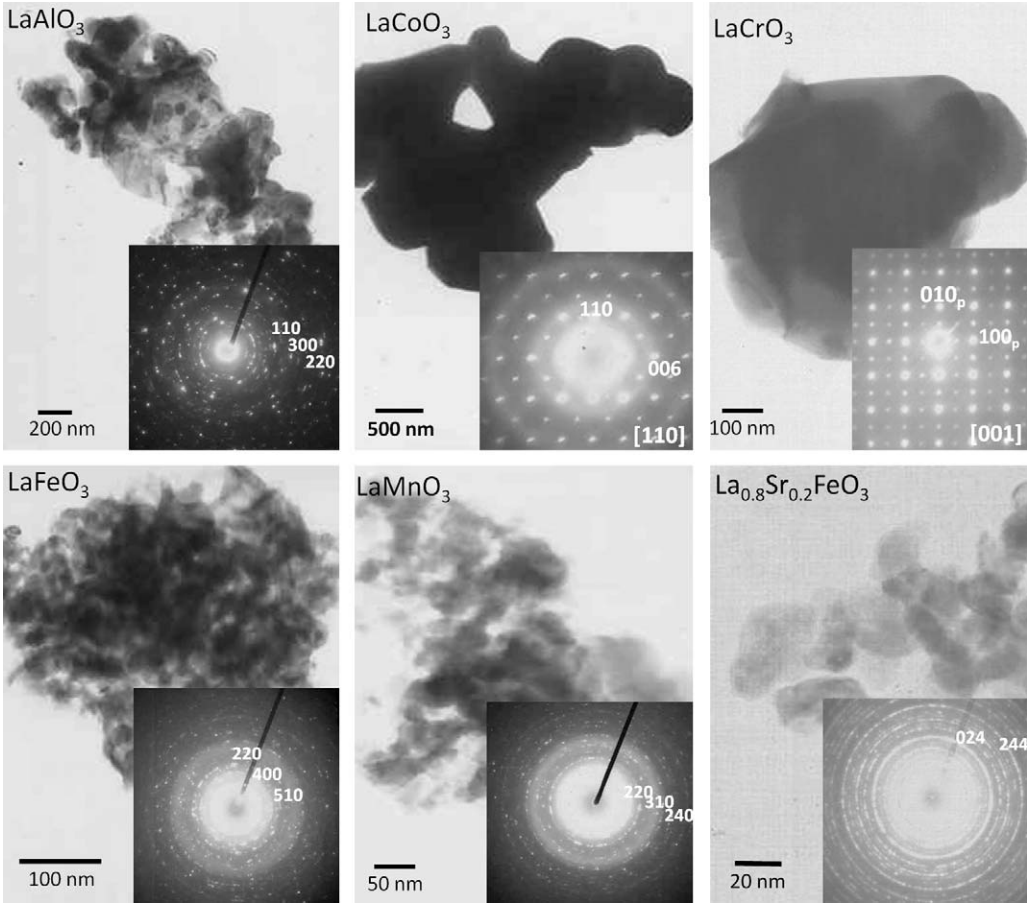

Fig. 7. TEM micrographs and SAED patterns of different lanthanum perovskites.

Table 4
TGA results for the reduction of Lanthanum perovskites in H_2.

$LaMO_{3\pm\delta}$	Intermediate products	Final products	% Weight loss	Composition
Cr	–	$LaCrO_3$	0.40	$LaCrO_{3.00(3)}$
Mn	$LaMnO_3$	$La_2O_3 + MnO$	4.06	$LaMnO_{3.12(1)}$
Fe	$La_2O_3 + FeO$	$La_2O_3 + Fe$	9.60	$LaFeO_{2.97(3)}$
Co	$La_2O_3 + CoO$	$La_2O_3 + Co$	9.69	$LaCoO_{2.99(2)}$
Sr, Fe	$La_2O_3 + SrO + FeO$	$La_2O_3 + SrO + Fe$	12.55	$La_{0.8}Sr_{0.2}FeO_{3.21(3)}$
Sr, Fe, Co	$La_2O_3 + SrO + FeO + CoO$	$La_2O_3 + SrO + Fe + Co$	12.52	$La_{0.8}Sr_{0.2}Fe_{0.5}Co_{0.5}O_{3.23(1)}$

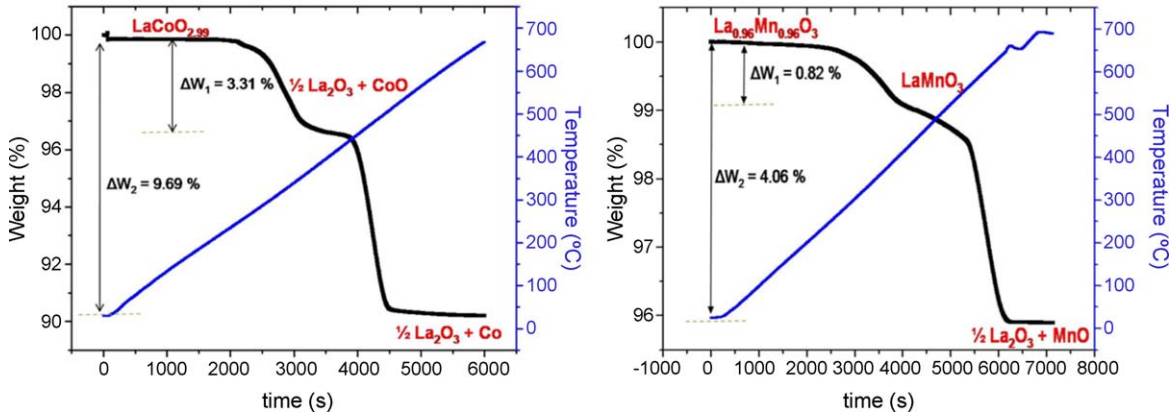

Fig. 8. Thermogravimetric plots corresponding to the H_2 reduction of $LaMnO_{3.12}$ and $LaCoO_3$.

highly agglomerated particles (Fig. 7). It can be observed that $LaCrO_3$ and $LaCoO_3$ have an average size of about 1 μm. However, the other perovskites are clearly in the nanometric range, e.g. the smaller particles are found for $LaMnO_3$ with an average size of 25 nm. The corresponding SAED patterns (insets of Fig. 7) show the diffraction rings commonly observed in nanocrystalline materials. $LaCoO_3$ diffraction can be indexed in the $[1\ 1\ 0]_p$ zone axis, and for $LaCrO_3$, electron diffraction patterns suggest the presence of a more complicated situation. The SAED pattern shown for $LaCrO_3$ presents a series of strong spots that can be indexed on the basis of the $[0\ 0\ 1]_p$ axis of a simple perovskite cell. This is the substructure common to these types of materials. Besides, one can also observe some extra spots at (1/2,1/2,0) which suggests the presence of a diagonal cell; characteristic of many perovskite superstructures, is associated to octahedral tilting and corresponding to a 3D-microdomain structure [36,37].

3.3. Oxygen contents

As explained above, the oxygen contents have been determined by performing thermogravimetric analysis in a hydrogen atmosphere. Table 4 shows the analysis of the reduction products and the weight loss together with the cationic stoichiometry data for all perovskites synthesized. Thermogravimetric reduction plots corresponding to $LaMnO_{3.12}$ and $LaCoO_3$ are presented in Fig. 8. Two different steps in the reduction process are apparent. In $LaMnO_{3.12}$, between 300 and 550 °C, manganites with different oxygen contents have been isolated. Above this temperature, the perovskite starts to decompose into La_2O_3 and MnO. In the case of $LaCoO_3$, the first step corresponds to the reduction to La_2O_3 and CoO between 300 °C to 450 °C. After that, it decomposes to the corresponding La_2O_3 and metallic Co. There is not a loss of weight in the case of stoichiometry $LaCrO_3$ in the measurement range below 700 °C. In the case of $La_{0.8}Sr_{0.2}FeO_3$ and $La_{0.8}Sr_{0.2}Fe_{0.5}Co_{0.5}O_3$ there are different reduction steps to La_2O_3, SrO and metallic Fe and/or Co.

3.4. Magnetic properties

Fig. 9 illustrates the susceptibility measurements of the different materials as a function of temperature in zero field cooling (ZFC) and field cooling (FC).

$LaCrO_3$ has an antiferromagnetic structure with a Neel temperature [T_N] of 280 K, as it is described in Refs. [38–40]. Therefore, the susceptibility values are quite small and the divergence between the ZFC and FC curves starts at room temperature. In $LaMnO_3$ the behavior is completely different and a broad paramagnetic–ferromagnetic transition is evident at $T_c \sim 170$ K. The actual composition is $LaMnO_{3.12}$, meaning that around 25% of Mn^{4+} is present, either if we formulate this material as oxygen-rich or if we consider cationic vacancies and write the formula as $La_{0.96}Mn_{0.72}{}^{3+}\ Mn_{0.24}{}^{4+}O_3$. The ferromagnetism of $LaMnO_{3+\delta}$ and its dependence on excess oxygen concentration, can be understood with the help of the theory of "double exchange interaction" proposed by Zener [41]. When the oxygen concentration increases in $LaMnO_3$, a corresponding number of Mn^{3+} ions are replaced by Mn^{4+} ions. The Mn^{4+} ion has the tendency to capture an electron from the Mn^{3+} ion. In our sample, the transition temperature [T_c] from ferromagnetic to paramagnetic reproduces well which has been described in the literature [42]. $LaCoO_3$ exhibits paramagnetic behavior in the intermediate/high spin states, whereas the low spin state is believed to be diamagnetic [43]. The maximum in susceptibility vs temperature near 85 K reflects a conversion of the remaining high spin Co^{3+} ions to diamagnetic low spin Co^{3+}. The sharp minimum at 25 K reflects the retention of some high spin cobalt ions to lowest temperatures. This behavior for $LaCoO_3$ was described by Señaris-Rodríguez and Goodenough in Ref. [44]. For $LaFeO_3$ the variation of χ_m does not obey the Curie or Curie–Weiss law which rules out the presence of any dominating paramagnetic phase. This material has been described as G-type antiferromagnetic due to the ordering of Fe^{3+}, ions, with a weak ferromagnetic component, due to spin canting with order temperatures close to 750 K [45,46]. In our case, this

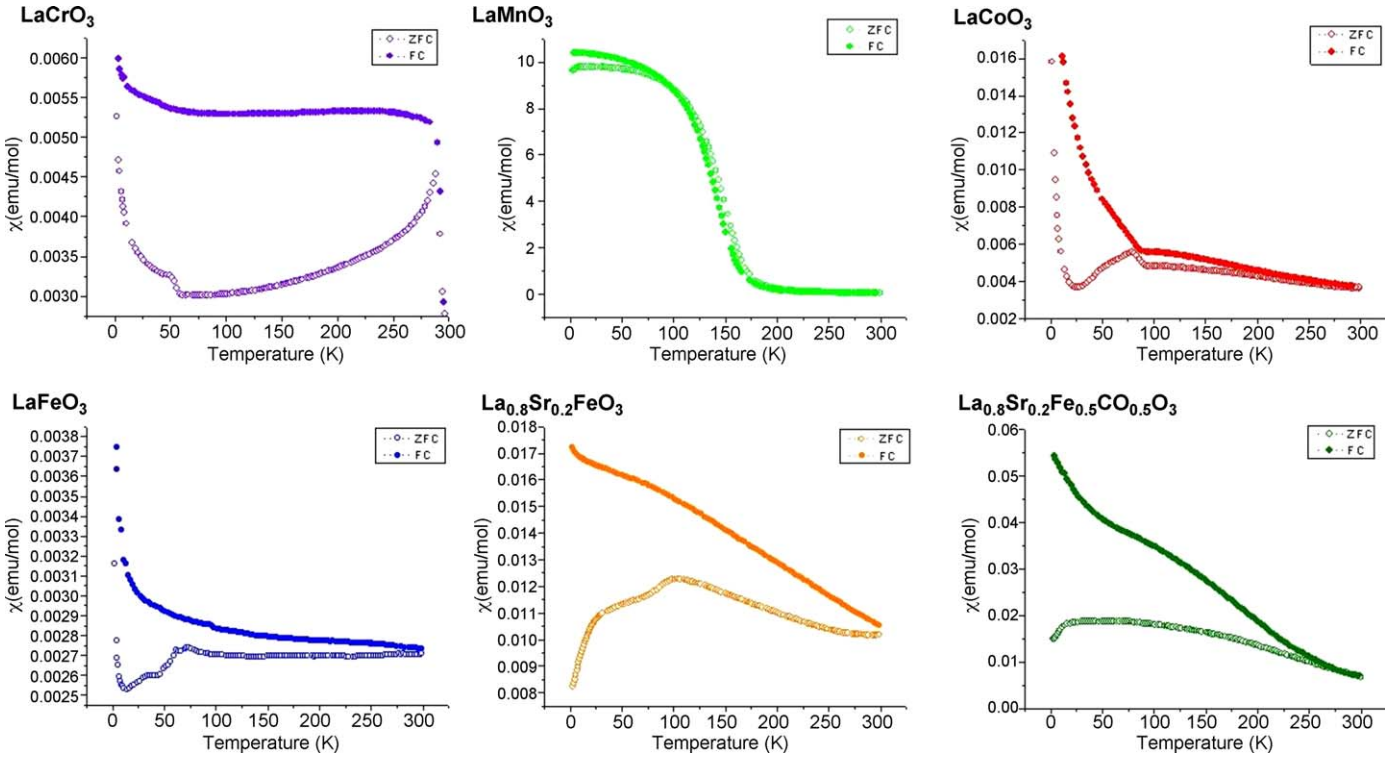

Fig. 9. Molar magnetic susceptibility measurements vs temperature of different lanthanum perovskites.

weak ferromagnetism component causes the divergence between ZFC and FC curves below room temperature. For Sr-doped materials an analogous behavior is observed although these curves diverge at lower temperatures probably due to the presence of some Fe^{4+} breaking the AFM superexchange coupling between Fe^{3+} ions. With all of this, we can say that both the microstructural features as well as the bulk properties, i.e. the general behavior of these perovskites are well preserved, which turns the microwave synthesis into a reliable, cheap and fast method for technologically important materials.

3.5. Electrical characterization

Preliminary electrochemical tests performed on the SOFCs cathodic materials: $LaMnO_3$, $LaFeO_3$ and $La_{0.8}Sr_{0.2}FeO_3$, reveal polarization resistances which are in agreement with reported data for these materials when obtained by other synthetic routes [47,48]. Activation energies range from 55 kJ mol^{-1} for the manganite to approximately 200 kJ mol^{-1} for the undoped ferrite. The polarization values of the lanthanum ferrite are rather high compared to Sr substituted material. Further work is in progress.

4. Conclusion

Some selected lanthanum perovskites have been successfully prepared by a fast and easy route of synthesis: microwave irradiation. This very simple method yields well crystallized and pure materials, sometimes nanosized, either in a single step synthesis or after further annealing. High density pellets can be produced after sintering at 1300 °C. The quality of the samples permits us to refine the structure by Rietveld method, something usually difficult for materials obtained by "fast" methods of synthesis. Magnetic and electric measurements have been compared with literature data and the values obtained are similar to those previously reported showing, at least in this case, that microwave-assisted synthesis is an interesting alternative.

Acknowledgements

The authors are gratefully indebted to CAM (Materyener P2009/PPQ-1626) and Spanish Micinn (MAT-2007-64006) for providing financial support.

References

[1] M. Backhaus-Ricoult, Solid State Sci. 10 (2008) 670.
[2] Y. Choi, D.S. Mebane, M.C. Lin, M. Liu, Chem. Mater. 19 (7) (2007) 1690.
[3] S. Petrovic, A. Terlecki-Baricevic, L. Karanovic, P. Kirilov-Stefanov, M. Zdujic, V. Dondur, D. Paneva, I. Mitov, V. Rakic, Appl. Catal. B: Environ. 79 (2008) 186.
[4] C. Vázquez-Vázquez, J. Mater. Res. 13 (1) (1998) 451.
[5] G. Shabbir, A.H. Qureshi, K. Saeed, Mater. Lett. 60 (2006) 3706.
[6] X. Qi, J. Zhou, Z. Yue, Z. Gui, L. Li, Mater. Chem. Phys. 78 (2002) 25.
[7] W. Zheng, R. Liu, D. Peng, G. Meng, Mater. Lett. 43 (2000) 19.
[8] K.E. Gibbons, M.O. Jones, S.J. Blundell, K.E. Gibbons, M.O. Jones, S.J. Blundell, A.I. Mihut, I. Gameson, P.P. Edwards, Y. Miyazaki, N.C. Hyatt, A. Porch, Chem. Commun. (2000) 159.
[9] M. Panneerselvam, K.J. Rao, J. Mater. Chem. 13 (2003) 596.
[10] A. Kaddouri, S. Ifrah, Catal. Commun. 7 (2006) 109.
[11] S. Farhadi, Z. Momeni, M. Taherimehr, J. Alloys Compd. 471 (2009) L5.
[12] H.M. Kingston, S.J. Haswell, Microwave-enhanced Chemistry, American Chemical Society Publication, 1997, p. 6.
[13] A.S. Kulkarni, R.V. Jayaram, Appl. Catal. A. Gen. 252 (2003) 225.
[14] S. Cho, S.-H. Jung, K.-H. Lee, J. Phys. Chem. C 112 (2008) 12769.
[15] Y.-J. Zhu, W.-W. Wang, R.-J. Qi, X.-L. Hu, Angew. Chem. Int. 43 (2004) 1410.
[16] D.R. Baghurst, A.M. Chippindale, D.M.P. Mingos, Nature 332 (1988) 311.
[17] D.R. Baghurst, D.M.P. Mingos, J. Chem. Soc., Chem. Commun. (1988) 829.
[18] D.M.P. Mingos, D.R. Baghurst, Chem. Soc. Rev. 20 (1991) 1.
[19] K.J. Rao, B. Vaidhyanathan, M. Ganguli, P.A. Ramakrishnan, Chem. Mater. 11 (4) (1999) 882.
[20] D.E. Clark, D.C. Folz, C. Folgar, M. Mahmoud, Microwave Solutions for Ceramic Engineers, American Ceramic Society, Westerville, OH, 2005.
[21] C.Y. Fang, C.A. Randan, M.T. Lanagan, D.K. Agrawal, J. Electroceram. 22 (2009) 125.
[22] .K. Sahu, M.L. Rao, S.S. Manoharan, J. Mater. Sci. 36 (2001) 4099.
[23] M. Gupta, W.W. Leong, Microwaves Metals, John Wiley & Sons, Asia, 2007, 35.
[24] J. Prado-Gonjal, M.E. Villafuerte-Castrejón, L. Fuentes, E. Morán, Mater. Res. Bull. 44 (8) (2009) 1734.
[25] C. Parada, E. Morán, Chem. Mater. 18 (11) (2006) 2719.
[26] S. Liu, X. Quian, J. Xiao, J. Sol–Gel Sci. Technol. 44 (2007) 187.
[27] R.D. Shannon, C.T. Prewitt, Acta Cryst. B25 (1969) 925.
[28] A.D. Jadhav, A.B. Gaikwad, V. Samuel, V. Ravi, Mater. Lett. 61 (2007) 2030.
[29] H. Taguchi, S.-I. Matsu-ura, M. Nagao, H. Kido, Physica B 270 (1999) 325.
[30] V.G. Sathe, S.K. Paranjpe, V. Siruguri, A.V. Pimpale, J. Phys.: Condens. Matter 10 (1998) 4045.

[31] S.E. Dann, D.B. Currie, M.T. Weller, M.F. Thomas, A.D. Al Rawwas, J. Solid State Chem. 109 (1994) 134.
[32] A. Wolf, R.J. Arnott, J. Phys. Chem. Solids J3 (1959) 176.
[33] A.P. Ramirez, J. Phys.: Condens. Matter 9 (1997) 8171.
[34] R.H. Mitchell. Perovskites Modern and Ancient, vol. 57. Almaz Press Inc., Canada, 2002, 317 pp.
[35] E. Arendt, A. Maione, A. Klisinska, O. Sanz, M. Montes, S. Suarez, J. Blanco, P. Ruiz, Appl. Catal. A: Gen. 339 (2008) 1.
[36] M.H. Aguirre, R. Ruiz-Bustos, M.A. Alario-Franco, J. Mater. Chem. 13 (2003) 1156.
[37] A. Vegas, M. Vallet-Regí, J. Gonzalez-Calbet, M.A. Alario-Franco, Acta Cryst. B 42 (1986).
[38] W.C. Koehler, E.O. Wollan, J. Phys. Chem. Solids 2 (1957) 100.
[39] Kenji Ueda, Hitoshi Tabata, Tomoji Kawai, Science 280 (1998) 1064.
[40] J.J. Neumeier, H. Terashita, Phys. Rev. B 70 (2004) 214435.
[41] C. Zener, Phys. Rev. 82 (3) (1951) 403.
[42] A. Tiwari, K.P. Rajeev, J. Mater. Sci. Lett. 16 (1997) 521.
[43] R. Schmidt, J. Wu, C. Leighton, I. Terry, Phys. Rev. B 79 (2009) 125105.
[44] M.A. Señaris-Rodriguez, J.B. Goodenough, J. Solid State Chem. 116 (1995) 224.
[45] S. Acharya, J. Mondal, S. Ghosh, S.K. Roy, P.K. Chakrabarti, Mater. Lett. 64 (2010) 415.
[46] H. Watanabe, Science reports of the Research Institutes, Tohuku University. Ser. A, Physics, Chem. Metall. 8 (1956) 14.
[47] S.P. Jiang, W. Wang, Solid State Ionics 176 (15–16) (2005) 1351.
[48] W.G. Wang, M. Mogensen, Solid State Ionics 176 (5–6) (2005) 457.